Supporting Information

Tan and Kapoor 10.1073/pnas.1106748108

SI Materials and Methods

Förster Resonance Energy Transfer Sensor Substrate Sequence. The Aurora sensor uses KVNKIVKNRRTVAI as its substrate sequence (1). The Polo-like kinase (Plk) sensor uses LLLDSTLSINWD as its substrate sequence (1).

Cell Culture. The 293-Ampho cells were cultured in DMEM (Invitrogen), and human telomerase reverse transcriptase-retinal pigment epithelial 1 (hTERT-RPE1) cells were cultured in DMEM/F12 1:1 nutrient mix (Invitrogen), supplemented with 10% FBS (Atlanta Biologicals) and penicillin-streptomycin (100 U/mL and 100 μg/mL respectively) (Invitrogen), at 37 °C in a humidified atmosphere with 5% CO_2. Cell lines used for imaging are retroviral stable cell lines. Retroviruses were generated by transfecting 293-Ampho cells by calcium phosphate precipitation. hTERT-RPE1 cells then were infected by retrovirus with 4 μg/mL Polybrene (Sigma) and selected by puromycin (Sigma), G418 (Sigma), or blasticidin (Sigma).

RNAi transfections were carried out by using Invitrogen RNAi Max reagent following the manufacturer's instructions. Cells then were plated in either six-well plates for immunoblots or on No. 1.5 12-mm circular coverslips (Fisher Scientific) for immunofluorescence. For Aurora B RNAi experiments, hTERT-RPE1 cell lines expressing the Aurora Förster resonance energy transfer (FRET) sensor were transfected with Aurora B siRNA oligos (5′-AACGCGGCACUUCACAAUUGA-3′) (1). For INCENP RNAi experiments, hTERT-RPE1 cell lines expressing either mCherry-INCENP WT or T59E mutant were transfected with INCENP siRNA oligos (5′-UGACACGGAGAUUGCCAAC-3′) (2).

For monopolar cytokinesis (Fig. 4), coverslips were incubated in medium with kinesin-5 inhibitor S-Trityl-L-Cysteine (STLC) (2 μM; Sigma) dissolved in DMSO and ethanol (0.1%; solvent for purvalanol A; Pharmco-AAPER) for 5 h and then exchanged into medium with both 2 μM STLC (Sigma) and 30 μM of the cyclin-dependent kinase 1 inhibitor purvalanol A (Tocris Bioscience) dissolved in ethanol (3).

Live-Cell Imaging. hTERT-RPE1 cells were grown on 22 × 22 mm coverslips (no. 1.5; Fisher Scientific) coated with poly-D-lysine (Sigma) and were mounted in a Rose chamber in L15 imaging medium (Invitrogen) without phenol red. The medium was supplemented with 10% FBS. The imaging chamber was maintained at 35–37 °C by an air-stream stage incubator (Nevtek). The FRET sensor was imaged, and the data were processed as described previously (1, 4). For linescan projections of the emission ratio images, custom software was written in MATLAB (Mathworks). Briefly, emission ratios were calculated for intensities above background. The spindle axis was determined by connecting the two centrosomes of the cell, and the position of the midpoint between the two centrosomes was set to be zero. Emission ratios of pixels with the same position along the spindle elongation axis were averaged, and the SD was calculated. The linescan projection was generated by plotting the averaged emission ratio against position, with SD for the emission ratio at all positions.

For imaging the FRET sensors, cells that have both spindle poles within a 2-μm distance in the *z*-direction were imaged so as to reduce errors from stack averaging. For imaging sensors in the Aurora kinase inhibition experiment in Fig. 2, rose chambers with cells expressing FRET sensors were assembled with 0.1% DMSO (solvent for ZM447439) in imaging medium. Metaphase cells were found and tracked until anaphase onset, and then medium was replaced with imaging medium containing 10 μM ZM447439 (Chemie Tek) dissolved in DMSO. Cells then were imaged every 2 min for 12 min.

For imaging FRET sensors in other small-molecule inhibitors [i.e., ZM447439 (Chemie Tek) in Fig. 1 and SI figures and latrunculin B (Sigma) and BI2536 (5) in Fig. 1], rose chambers with cells expressing FRET sensors were assembled with 0.1% DMSO (solvent for ZM447439, latrunculin B, and BI2536) in imaging medium. In the case of ZM447439, cells were incubated with 0.3 μM inhibitor for 30 min and then were subjected to imaging. Metaphase cells that showed a clear metaphase plate and had both spindle poles within a 2-μm distance in the *z*-direction were imaged. For latrunculin B and BI2536 experiments, metaphase cells were located, and medium was replaced with imaging medium containing 2 μM latrunculin B or 250 nM BI2536. Anaphase cells were tracked for >20 min after anaphase onset.

For nearly simultaneous imaging of FRET sensors and mCherry-INCENP in live cells (Figs. 2 and 4), FRET sensors were imaged as above, using a 512B camera (Photometrics) mounted on the microscope side port. mCherry-INCENP images for the same cells were collected nearly simultaneously using epifluorescence on a separate HQ camera (Photometrics) mounted on the microscope's base port.

For GFP-anillin analysis in Fig. 4, hTERT-RPE1 cell lines stably expressing GFP-anillin, GFP-protein regulator of cytokinesis 1 (GFP-PRC1), and mCherry-INCENP WT or T59E were used. Confocal fluorescence images were acquired every 10 s using a Nikon TE2000 microscope (Morrell Instruments) with a PlanApo 100× NA 1.40 objective. Anaphase onset (time 0) was determined based on centromere separation in the mCherry-INCENP channel. The equatorial plane was determined by averaging the GFP-PRC1 localization from images at 330, 340, and 350 s. Linescans (width = 10 pixels) were generated for images from all time points. For each linescan profile, there are two peaks for GFP-anillin signal, corresponding to the two edges of the cell. The maximum GFP-anillin signal intensity *Ip* (for the equatorial GFP-anillin signal at each time point) was calculated by averaging three pixels, with the maximum-intensity pixel at the center, for each cell edge (i.e., averaging signal for a total of six pixels). The relative enrichment factor was calculated using the equation $[Ip(t) - Ip(t = 0)]/Ip(t = 0)$ and was plotted against time. These analyses were carried out using MATLAB.

Immunoblots. Cells were incubated in medium containing 10 μM nocodazole (Sigma) for 16 h before harvest. Cells then were lysed and subjected to SDS/PAGE followed by immunoblotting. Primary antibodies used in immunoblotting were anti-INCENP (AbCam), anti-cyclin B (BD Biosciences), and anti-protein phosphatase 2A (anti-PP2A) (Santa Cruz). IRDye 800 goat anti-rabbit or anti-mouse IgG (Li-Cor) was used according to the manufacturer's instructions. Blots were detected and quantified using the Odyssey Infrared Imaging System (Li-Cor).

Immunofluorescence Microscopy. Coverslips first were fixed for 10 min in 4% formaldehyde in PBS buffer at room temperature and then were incubated for 10 min in methanol at −20 °C. Subsequently, coverslips were washed with PBS and 0.5% Triton X-100 in PBS (PBS-tx). Washed coverslips were blocked in 5% BSA in PBS-tx for 30 min. Primary antibodies were incubated in 2% BSA in PBS-tx and were from the following sources: anti–Polo-like kinase 1 (anti-Plk1) (Santa Cruz); rabbit polyclonal anti-PRC1; Aurora B antibody (anti-AIM 1; Signal Transduction Laboratory); anti–mitotic kinesin-like protein 1 (MKLP1) (Santa

Cruz); and FITC-conjugated anti-tubulin DM1A (Sigma). DNA was stained with DAPI (Invitrogen). Secondary antibodies used were Dylight-conjugated donkey anti-rabbit and anti-mouse antibodies (Jackson Immunological Laboratories). For Ras homolog gene family member A (RhoA) visualization, cells were fixed with 10% trichloroacetic acid (Sigma) on ice for 10 min and stained with anti-RhoA (Santa Cruz). Images were acquired as Z stacks with 0.15-μm spacing using a 100×, 1.35 NA objective on a DeltaVision Image Restoration Microscope (Applied Precision Instruments and Olympus) and were processed by iterative constrained deconvolution (Softworx; Applied Precision Instruments). Maximal-intensity projections of the entire Z stack are shown. Linescans for immunofluorescence images were generated using ImageJ software. A line with 3.7-μm width was drawn by connecting the two spindle poles, and an averaged plot profile was generated.

1. Fuller BG, et al. (2008) Midzone activation of aurora B in anaphase produces an intracellular phosphorylation gradient. *Nature* 453:1132–1136.
2. Vader G, Kauw JJW, Medema RH, Lens SMA (2006) Survivin mediates targeting of the chromosomal passenger complex to the centromere and midbody. *EMBO Rep* 7:85–92.
3. Hu C-K, Coughlin M, Field CM, Mitchison TJ (2008) Cell polarization during monopolar cytokinesis. *J Cell Biol* 181:195–202.
4. Tseng BS, Tan L, Kapoor TM, Funabiki H (2010) Dual detection of chromosomes and microtubules by the chromosomal passenger complex drives spindle assembly. *Dev Cell* 18:903–912.
5. Steegmaier M, et al. (2007) BI 2536, a potent and selective inhibitor of polo-like kinase 1, inhibits tumor growth in vivo. *Curr Biol* 17:316–322.

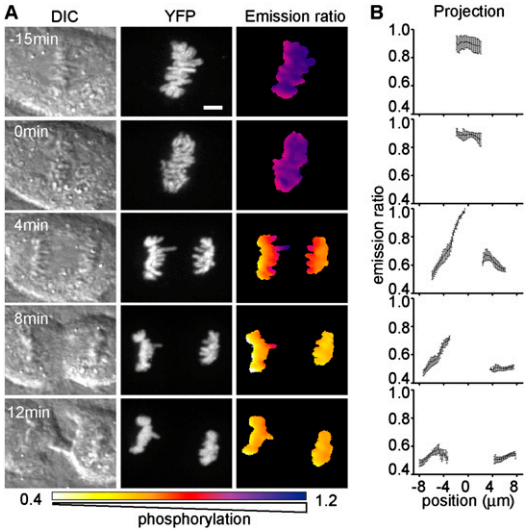

Fig. S1. The chromatin-targeted FRET sensor for Aurora kinase activity does not readily allow spatially continuous measurements of substrate phosphorylation during anaphase. (*A*) A cell expressing a chromatin-targeted FRET sensor is imaged through anaphase. Differential interference contrast (DIC), YFP, and color-coded emission ratio images are shown. (Scale bar, 5 μm.) (*B*) Corresponding linescan projections of emission ratios along the spindle elongation axis are shown. Time stamps are relative to anaphase onset. Error bars indicate SD.

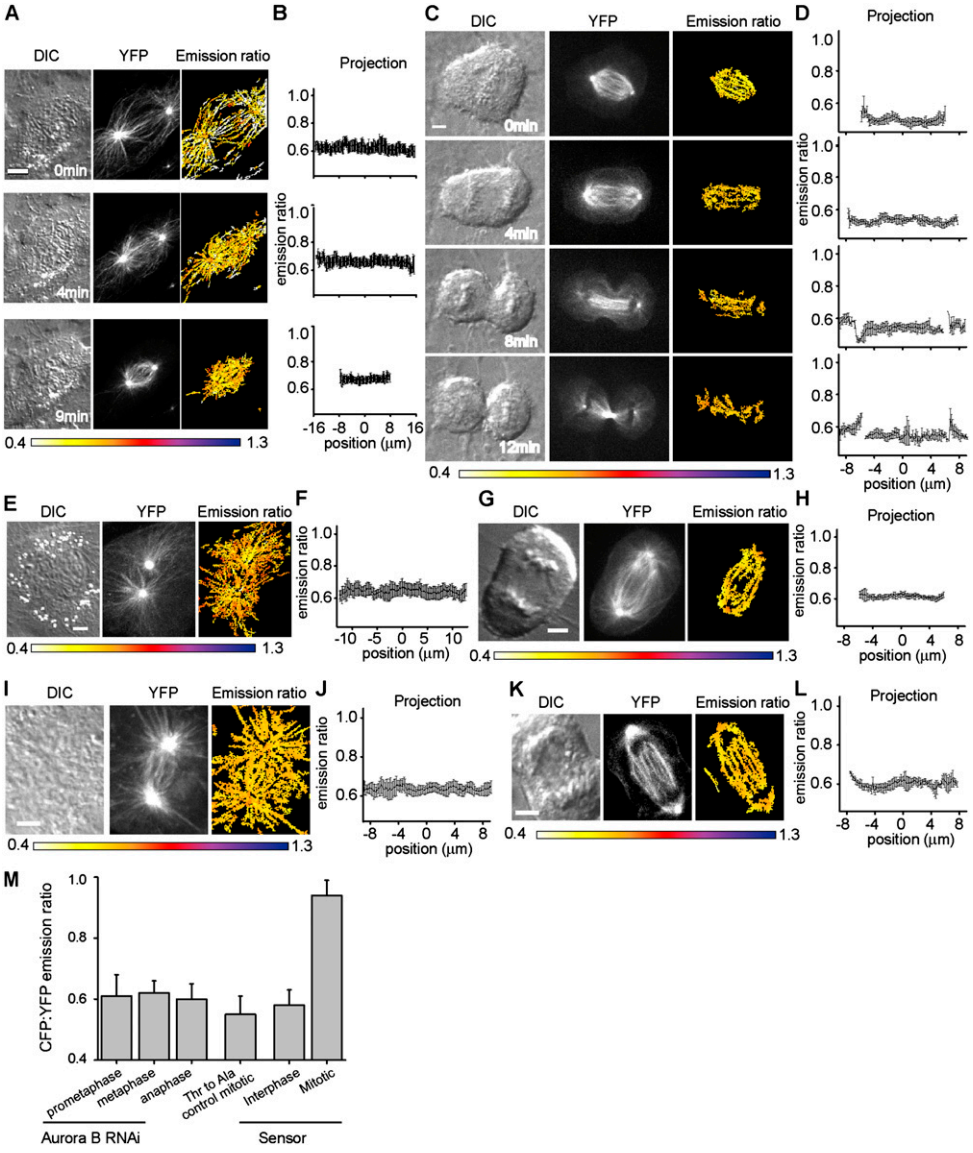

Fig. S2. Specificity analysis of the microtubule-targeted FRET sensor for Aurora kinase activity. (*A*–*D*) Cells expressing the microtubule-targeted sensor lacking the phospho-acceptor threonine (mutated to alanine) are imaged through prophase–prometaphase (*A*) and anaphase (*C*). DIC, YFP, and color-coded emission ratio images are shown. Corresponding linescan projections are shown in *B* and *D*. (*E*–*H*) A prometaphase cell (*E*) and an anaphase cell (*G*) expressing the microtubule-targeted sensor treated with Hesperadin (100 nM), an Aurora kinase inhibitor. DIC, YFP, and color-coded images of the CFP:YFP emission ratio are shown. Corresponding linescan projections are shown in *F* and *H*. (*I*–*L*) DIC, YFP, and color-coded images of the CFP:YFP emission ratio are shown of a prometaphase cell (*I*) and an anaphase cell (*K*) expressing the microtubule-targeted sensor in which Aurora B is depleted by RNAi. Corresponding linescan projections are shown in *J* and *L*. (*M*) Analysis of CFP:YFP emission ratios ($n > 10$ cells in each condition). Note that the data for sensor (no RNAi) and mutated sensor are provided for comparison and have been recalculated using datasets reported previously (1). Error bars indicate SD. (Scale bars, 5 μm.)

1. Tseng BS, Tan L, Kapoor TM, Funabiki H (2010) Dual detection of chromosomes and microtubules by the chromosomal passenger complex drives spindle assembly. *Dev Cell* 18:903–912.

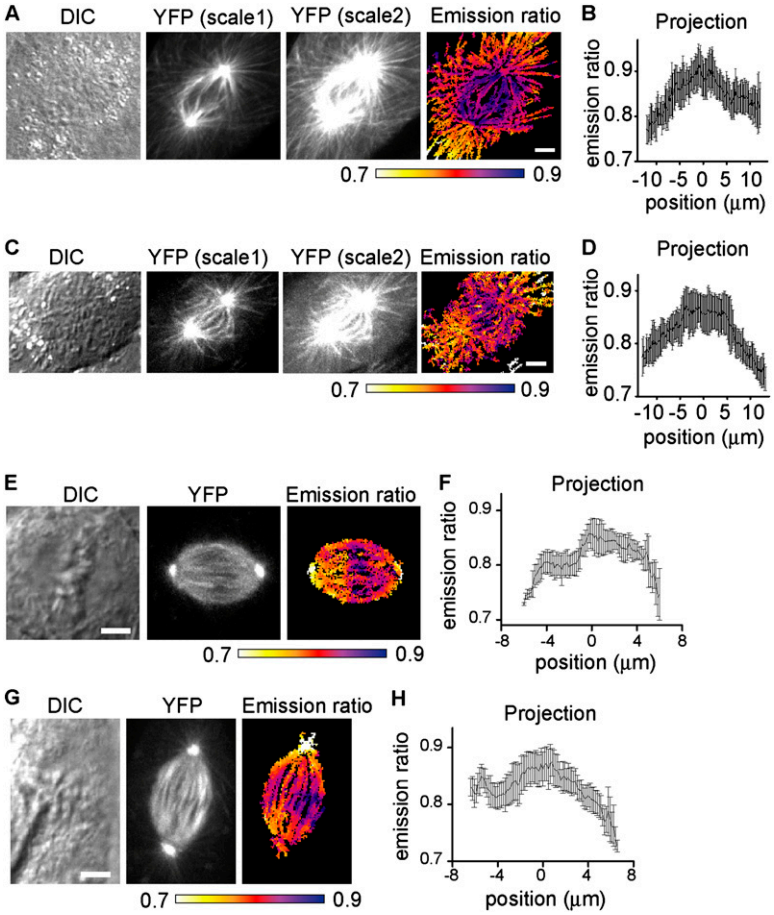

Fig. S3. Analysis of the microtubule-targeted FRET sensor for Aurora kinase activity in cells at prometaphase and in cells at metaphase that were treated with an Aurora kinase inhibitor, ZM447439 (0.3 μM). (*A*–*D*) Two prometaphase cells expressing the microtubule-targeted sensor were imaged live. DIC, YFP at two different intensity scales, and color-coded CFP:YFP emission ratio images are shown in *A* and *C*, and corresponding linescan projections are shown in *B* and *D*. (*E*–*H*) Two examples of ZM447439-treated metaphase cells in which the FRET sensor indicates an asymmetric phosphorylation pattern. DIC, YFP, and color-coded CFP:YFP emission ratio images are shown in *E* and *G*. Corresponding linescan projections are shown in *F* and *H*. Error bars indicate SD. (Scale bars, 5 μm.)

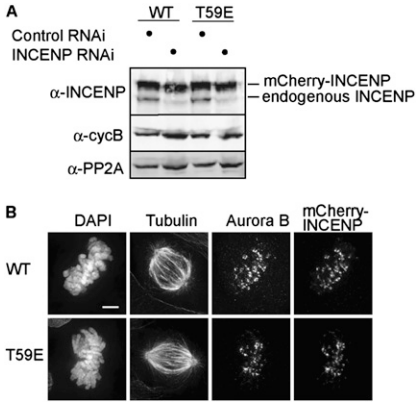

Fig. S4. Examining chromosomal passenger complex (CPC) localization in cells after INCENP knockdown and addback of the WT or T59E mutant of INCENP. (*A*) A representative Western blot showing knockdown of endogenous INCENP and expression of mCherry-INCENP constructs. Cyclin B (cycB) and PP2A are loading controls. (*B*) WT-addback and T59E-addback cells were fixed and stained to label chromosomes (DAPI), tubulin, Aurora B, and mCherry-INCENP. Preanaphase cells are shown here (anaphase cells are shown in Fig. 2). (Scale bar, 5 μm.)

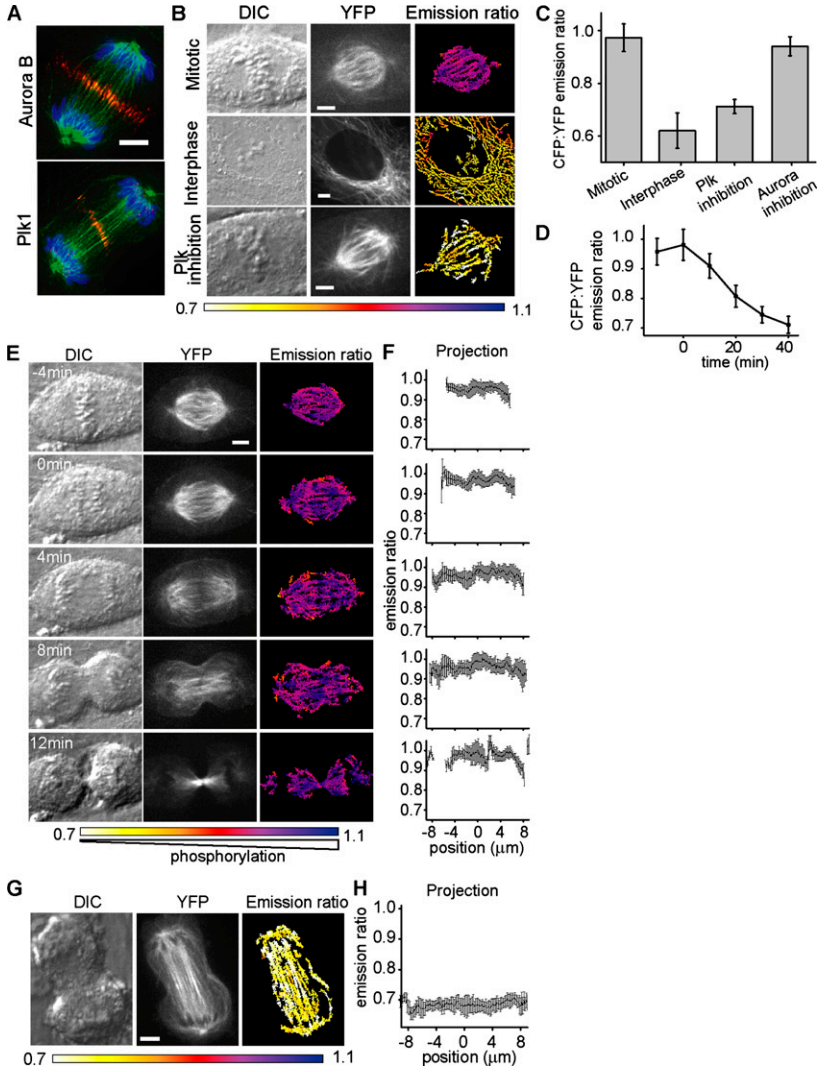

Fig. S5. Analysis of a microtubule-targeted FRET sensor for Plk1 activity. (*A*) Immunofluorescence images of Aurora B or Plk1 (red), tubulin (green), and DNA (blue). (*B*) Cells expressing the Plk FRET sensor imaged live. DIC, YFP, and CFP:YFP emission ratio images are shown. (*C*) Analysis of CFP:YFP emission ratios in mitosis and interphase for the Plk sensor (n = 30 cells) and for the sensor in mitosis after Plk inhibition by 100 nM BI2536 (n = 27 cells) or after Aurora inhibition by 2 μM ZM447439 (n = 30 cells). (*D*) Analysis of the Plk sensor in mitotic cells treated with 100 nM BI2536. Average CFP:YFP emission ratios are plotted against time (n = 10 cells). (*E* and *F*) Microtubule-targeted Plk sensor is imaged through anaphase. DIC, YFP, and emission ratio images are shown in *E*. Corresponding linescan projections are shown in *F*. Timestamps are relative to anaphase onset. (*G* and *H*) Images of cells expressing a microtubule-targeted Plk sensor with the phospho-acceptor threonine mutated to alanine. DIC, YFP, and emission ratio images are shown in *G*. Corresponding linescan projections are shown in *H*. Error bars indicate SD. (Scale bars, 5 μm.)

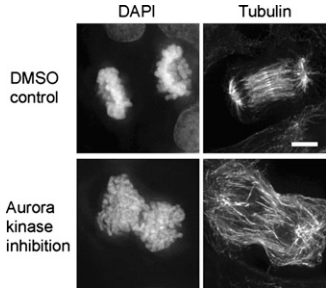

Fig. S6. Inhibition of CPC kinase activity disrupts anaphase spindle morphology. RPE1 cells treated with DMSO (0.1%) or an Aurora kinase inhibitor (Hesperadin; 100 nM) were fixed and stained for DNA (DAPI) and tubulin. (Scale bar, 5 μm.)

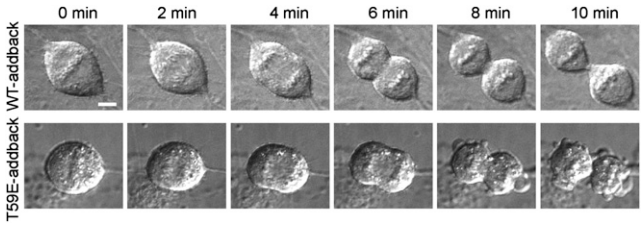

Fig. S7. Cleavage-furrow ingression in WT-addback and T59E-addback cells imaged through anaphase. DIC images are shown. (Scale bar, 5 μm.)

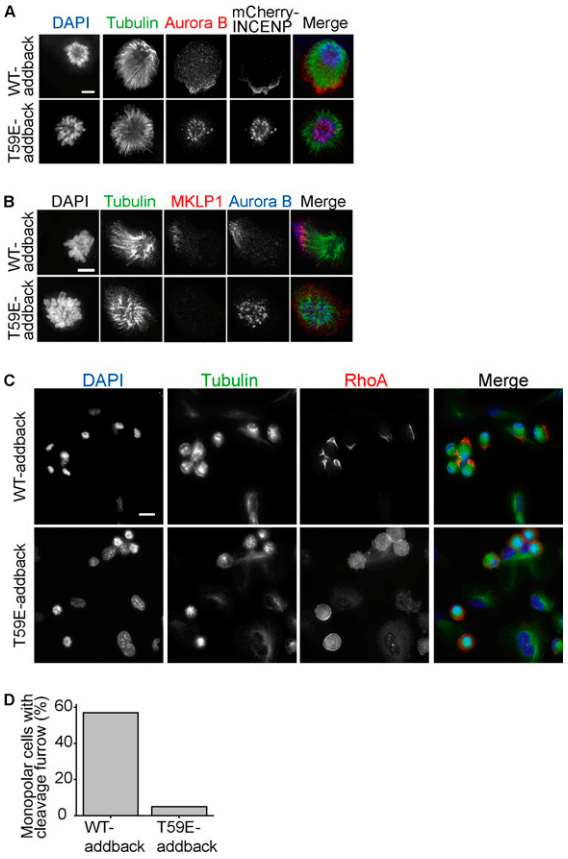

Fig. S8. Analysis of monopolar cytokinesis in T59E–addback cells. (*A*) WT-addback and T59E–addback cells undergoing monopolar cytokinesis were fixed and stained for chromosomes (DAPI, blue), tubulin (green), Aurora B (red), and mCherry-INCENP. (*B*) WT-addback and T59E–addback cells undergoing monopolar cytokinesis fixed and stained to label chromosomes (DAPI), tubulin (green), Aurora B (blue), and MKLP1 (red). (*C*) WT-addback and T59E–addback cells undergoing monopolar cytokinesis were fixed and stained for DNA (DAPI, blue), tubulin (green), and RhoA (red). (*D*) Percentage of WT-addback cells (n = 70) and T59E–addback cells (n = 56) undergoing monopolar cytokinesis and having assembled cleavage furrows. (Scale bars, 5 μm.)